Neurobiology of Disease 178 (2023) 106030

Contents lists available at ScienceDirect

Neurobiology of Disease

journal homepage: www.elsevier.com/locate/ynbdi

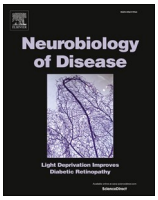

Identification of a novel pathway in sporadic Amyotrophic Lateral Sclerosis mediated by the long non-coding RNA ZEB1-AS1

Federica Rey [a,1], Erika Maghraby [a,b,1], Letizia Messa [c,d], Letizia Esposito [a], Bianca Barzaghini [e], Cecilia Pandini [f], Matteo Bordoni [g], Stella Gagliardi [h], Luca Diamanti [i], Manuela Teresa Raimondi [e], Massimiliano Mazza [j], Gianvincenzo Zuccotti [a,k], Stephana Carelli [a,2,*], Cristina Cereda [c,2]

[a] Pediatric Research Center "Romeo ed Enrica Invernizzi", Department of Biomedical and Clinical Sciences, University of Milan, Milan, Italy
[b] Department of Biology and Biotechnology "L. Spallanzani", University of Pavia, Pavia, Italy
[c] Center of Functional Genomics and Rare Diseases, Department of Pediatrics, Buzzi Children's Hospital, Milan, Italy
[d] Department of Electronics, Information and Bioengineering (DEIB), Politecnico di Milano, Milan, Italy
[e] Department of Chemistry, Materials and Chemical Engineering "Giulio Natta", Politecnico di Milano, Milan, Italy
[f] Department of Biosciences, University of Milan, Milan, Italy
[g] Cellular Models and Neuroepigenetics Unit, IRCCS Mondino Foundation, Pavia, Italy
[h] Molecular Biology and Transcriptomics Unit, IRCCS Mondino Foundation, Pavia, Italy
[i] Neuroncology Unit, IRCCS Mondino Foundation, Pavia, Italy
[j] Immunotherapy, Cell Therapy and Biobank (ITCB), IRCCS Istituto Romagnolo per lo Studio dei Tumori (IRST) "Dino Amadori", Meldola, Italy
[k] Department of Pediatrics, Buzzi Children's Hospital, Milan, Italy

ARTICLE INFO

Keywords:
ZEB1-AS1
hsa-miR-200c
Long non-coding RNA
Amyotrophic Lateral Sclerosis
cancer
Neurodegeneration
Neuronal differentiation
β-Catenin

ABSTRACT

Background: Deregulation of transcription in the pathogenesis of sporadic Amyotrophic Lateral Sclerosis (sALS) is taking central stage with RNA-sequencing analyses from sALS patients tissues highlighting numerous deregulated long non-coding RNAs (lncRNAs). The oncogenic lncRNA ZEB1-AS1 is strongly downregulated in peripheral blood mononuclear cells of sALS patients. In addition, in cancer-derived cell lines, ZEB1-AS1 belongs to a negative feedback loop regulation with hsa-miR-200c, acting as a molecular sponge for this miRNA. The role of the lncRNA ZEB1-AS1 in sALS pathogenesis has not been characterized yet, and its study could help identifying a possible disease-modifying target.

Methods: the implication of the ZEB1-AS1/ZEB1/hsa-miR-200c/BMI1 pathway was investigated in multiple patients-derived cellular models (patients-derived peripheral blood mononuclear cells and induced pluripotent stem cells-derived neural stem cells) and in the neuroblastoma cell line SH-SY5Y, where its function was inhibited via RNA interference. Molecular techniques such as Real Time PCR, Western Blot and Immunofluorescence were used to assess the pathway dysregulation.

Results: Our results show a dysregulation of a signaling pathway involving ZEB1-AS1/hsa-miR-200c/β-Catenin in peripheral blood mononuclear cells and in induced pluripotent stem cells-derived neural stem cells from sALS patients. These results were validated in vitro on the cell line SH-SY5Y with silenced expression of ZEB1-AS1. Moreover, we found an increase for ZEB1-AS1 during neural differentiation with an aberrant expression of β-Catenin, highlighting also its aggregation and possible impact on neurite length.

Abbreviations: AD, Alzheimer's disease; ALS, Amyotrophic lateral sclerosis; C9orf72, Chromosome 9 Open Reading Frame 72; CTR, healthy controls; EMT, epithelial-to-mesenchymal transition; FUS, fused in sarcoma; GSK3β, Glycogen synthase kinase 3β; lncRNAs, long non-coding RNAs; PBMCs, Peripheral Blood Mononuclear Cells; PD, Parkinson's Disease; RA, retinoic acid; SEM, Standard Error Mean; Ser9, serine 9; SOD1, superoxide dismutase 1; TARDBP, TAR DNA-binding protein 43; Tyr216, tyrosine 216; ZEB1-AS1, Zinc finger *E*-box binding homeobox 1 antisense 1.

* Corresponding author at: Pediatric Clinical Research Center Fondazione "Romeo ed Enrica Invernizzi", Department of Biomedical and Clinical Sciences, University of Milan, Milan, Italy.
E-mail address: stephana.carelli@unimi.it (S. Carelli).
[1] These authors contributed equally to the work.
[2] These authors contributed equally to the work.

https://doi.org/10.1016/j.nbd.2023.106030
Received 11 October 2022; Received in revised form 17 January 2023; Accepted 30 January 2023
Available online 2 February 2023

Conclusions: Our results support and describe the role of ZEB1-AS1 pathway in sALS and specifically in neuronal differentiation, suggesting that an impairment of β-Catenin signaling and an alteration of the neuronal phenotype are taking place.

1. Background

Amyotrophic Lateral Sclerosis (ALS) is a progressive neurodegenerative disorder characterized by both upper and lower motor neurons loss in the spinal cord, brainstem and motor cortex (Recabarren-Leiva and Alarcón, 2018). Neuronal degeneration leads to muscular atrophy and spasticity which evolves to paralysis within 3–5 years from the onset of symptoms and usually culminates with death by respiratory failure (Robberecht and Philips, 2013). So far, there is no primary therapy for ALS with a very limited number of drugs being approved by the US Food and Drug Administration for disease treatment, including Riluzole, a glutamate antagonist whose mechanism of action is still unclear, and Edaravone in US and Japan (Jackson et al., 2019; Bensimon et al., 1994). As in other neurodegenerative diseases, the exact molecular pathway causing motor neuron degeneration in ALS is still unknown, probably because it is based on the involvement of a complex interplay between different cellular mechanisms such as mitochondrial impairment, protein aggregation and excitotoxicity (Robberecht and Philips, 2013). Whilst the vast majority of ALS cases do not present specific gene mutations, 22 genes have been associated with ALS, including Chromosome 9 Open Reading Frame 72 (C9orf72), superoxide dismutase 1 (SOD1), TAR DNA-binding protein 43 (TARDBP) and fused in sarcoma (FUS) (Van Damme et al., 2017). Notably, TARDBP and FUS are involved in multiple aspects of RNA metabolism, suggesting that coding and non-coding RNA and RNA expression deregulation may be key aspects in the pathogenesis of ALS (Garofalo et al., 2020).

LncRNAs are found to be deregulated in numerous physiological and pathological contexts, highlighting their relevance in the pathogenesis of several diseases (Riva et al., 2016; Carelli et al., 2019; Lyu et al., 2019; Rey et al., 2021a; Rey et al., 2021b; Rey et al., 2021c). A screening study was recently performed identifying RNA-dysregulation in Peripheral Blood Mononuclear Cells (PBMCs) from sporadic ALS (sALS) patients versus healthy controls, highlighting a strong deregulation in lncRNAs expression (Gagliardi et al., 2018). Specifically in ALS pathogenesis, genome-wide analyses of the human transcriptome have revealed multiple lncRNAs whose biogenesis, regulation, and cellular roles are modified (Rey et al., 2021d). Examples of lncRNAs involved in ALS pathogenesis include PAXBP-AS1, the antisense transcript of a PAXBP which encodes for a protein instrumental for skeletal muscle development, and NEAT1, which is mainly expressed in spinal motoneurons at the early stage of ALS and binds to TDP-43 factor in the brain (Wu and Kuo, 2020).

Amongst the top ten deregulated lncRNAs identified in the above cited study, three were antisense of transcription-related genes: *ZEB1-AS1*, the antisense of *ZEB1* gene; *ZBTB11-AS1,* the antisense of *ZBTB11* gene; and Xbac-BPG252P9.10, the antisense of IER3 gene (Gagliardi et al., 2018). In particular, the lncRNA Zinc finger *E*-box binding homeobox 1 antisense 1 (ZEB1-AS1) is a lncRNA predominantly known for its role in multiple cancers (Li et al., 2018; Li et al., 2016; Li et al., 2017). *ZEB1-AS1* is located on chromosome 10p11.22 (Li et al., 2017) and it is transcribed from a shared bi-directional promoter with *ZEB1* (Li et al., 2016). Physiologically, *ZEB1* encodes for a protein that has 7 zinc fingers and 1 homeodomain which regulates an important transcriptional network necessary for cell differentiation and self-renewal (Wu et al., 2020). Indeed, it is a prime element of a network of transcription factors that control epithelial-to-mesenchymal transition (EMT) (Li et al., 2019). ZEB1 was also found to exert a significant role in the regulation of important tumor features such as invasion and proliferation (Wu et al., 2020).

ZEB1-AS1 expression is directly associated with increased *ZEB1* gene expression in multiple cancers where it promotes an invasive phenotype (Siena et al., 2019). A possible mechanism of action includes the binding of hsa-miR-200c to ZEB1-AS1 that acts as sponge in competition for the binding of ZEB1 mRNA. Although the first pathogenic driver between ZEB1-AS1 and hsa-miR-200c has not been identified, this mechanism prevents thereby ZEB1 mRNA degradation promoting the recruitment of the H3K4 methyltransferase p300 and a chromatin status shift from inactive to active state facilitating also the ZEB1 transcription (Meng et al., 2018).

ZEB1-AS1 action as a sponge for hsa-miR-200c leads to the upregulation of BMI1, an oncogene member of the polycomb group gene family and a transcriptional repressor (Su et al., 2017). Overexpression of BMI1 has been identified in various human cancers, suggesting its involvement in cancer cell proliferation, invasion, distant metastasis, chemosensitivity and correlation with patient survival (Su et al., 2017). Interestingly, in the context of neurodegenerative diseases it has been reported that BMI1 deficiency leads to overexpression of Glycogen Synthase Kinase 3β (GSK3β) and to its phopshorylation (p-GSK3β) in human post-mitotic neuronal cells in brain of late-onset sporadic Alzheimer's disease (AD) (Hu et al., 2009). Dysregulation of GSK3β activity in neurons has been implicated in the pathogenesis of many neurodegenerative diseases such as AD, Parkinson's Disease (PD) and ALS (Armentero et al., 2011; Gianferrara et al., 2022). In different experimental models, the Wnt/β-Catenin canonical pathway has been demonstrated to regulate the self-renewal of neural progenitor cells and neuronal differentiation in the developing neocortical ventricular zone (Yang, 2012), subcortical areas of the telencephalon (Mutch et al., 2010), and ventral midbrain (Wang et al., 2017). Typically, in the absence of Wnt ligands GSK-3 acts together with β-Catenin and Adenomatous Polyposis Coli (APC) to bind the scaffolding protein Axin thus facilitating the phosphorylation of β-Catenin by GSK-3, leading to its proteasome-dependent degradation. The binding of Wnt to its ligands ultimately leads to GSK-3 inhibition and thus β-Catenin stabilization (Valvezan and Klein, 2012). Deregulation of Wnt/β-Catenin pathway has been related to several neurodegenerative disorders including AD (Jia et al., 2019), PD (Marchetti et al., 2020) and ALS, where it was found to aggregate in motor neuron somas of pre-symptomatic mutant SOD1 mice (Pinto et al., 2019).

Taken together this evidence points to the ZEB1-AS1/hsa-miR-200c/BMI1 pathway as a potential crucial regulator also in neurodegeneration. For this reason, the main aim of this experimental work is to investigate the mechanism of action of the antisense lncRNA ZEB1-AS1 in sALS, focusing on its impact on the hsa-miR-200c/BMI1 pathway and on the neuronal phenotype.

2. Material and methods

2.1. PBMCs isolation

PBMCs were immediately isolated from peripheral venous blood by sALS patients ($N = 10$) and healthy subjects ($N = 10$) using Histopaque®-1077 (Sigma-Aldrich) following the manufacturer's instructions. Briefly, PBMCs were prepared by centrifugation layering peripheral blood on Ficoll-Histopaque (density = 1.077) and centrifuged at 950*g* for 30 min.

PBMCs were collected from each subject and processed for Real-Time PCR and Western Blotting Analysis (see sections below).

2.2. PBMCs reprogramming

5×10^5 PBMCs from 1 sALS patients and 1 healthy control were resuspended in 24-well plates with PBMCs medium (StemPro™-34 + SCF 100 ng/ml, FLT-3100 ng/ml, IL-3 20 ng/ml, IL-6 20 ng/ml) (Fantini et al., 2019). Viruses provided by CytoTune®-iPS 2.0 Sendai Reprogramming Kit (Thermo Fisher Scientific) were incubated for 24 h. The medium was replaced with fresh complete PBMCs medium to remove the CytoTune™ 2.0 Sendai reprogramming vectors. After 2 days, cells were plated on vitronectin-coated culture dishes in complete StemPro™-34 medium (Thermo Fisher Scientific), the consumed medium was replaced every day for 4 days. 7 days after transduction, cells were grown in Essential 8 Medium (Thermo Fisher Scientific), and consumed medium was replaced every two days for 3 weeks. Undifferentiated colonies were manually picked and plated on vitronectin-coated well. Then, colonies were split using 0.5 mM EDTA for 3–5 passages. Efficient reprogramming was assessed by immunofluorescence analysis of stemness markers, using Pluripotent Stem Cell 4-Marker Immunocytochemistry Kit (Thermo Fisher Scientific), containing anti-SSEA4, anti-OCT4, anti-SOX2, and anti-TRA 1–60, following manufacturer's instructions. Specifically, cells were incubated with 4% PFA at room temperature and permeabilized with saponin 1%. After incubation with blocking solution, primary antibodies were added and cells were incubated overnight at 4 °C. Cells were rinsed with wash buffer and secondary antibodies were added at room temperature. Samples were washed, mounted with NucBlue® Fixed Cell Stain (DAPI) (Thermo Fisher Scientific), dried, nail-polished, and analyzed by confocal microscopy. iPSCs characterization is reported in (Carelli et al., 2019; Scarian et al., 2022).

2.3. Neural stem cells differentiation from induced pluripotent stem cells

The differentiation protocol of induced Pluripotent Stem Cells (iPSCs) into Neural Stem Cells (NSCs) is based on PSC Neural Induction Medium (Thermo Fisher Scientific) (Fantini et al., 2019). iPSCs at 5th passage were seeded in 6-well plate and coated with vitronectin. When cells reached about 70% confluency, the medium was changed from Essential 8 to Neurobasal (Thermo Fisher Scientific) supplemented with Neural Induction Supplement 50× (Thermo Fisher Scientific) for 7 days refreshing the medium daily. After 7 days, the iPSCs were differentiated into NSCs, obtaining a mixed neural population (Scarian et al., 2022). Cells were then split using StemPro Accutase (Thermo Fisher Scientific) to expand cells and cryopreserved for further differentiation protocol. The same protocol used for efficient reprogramming assessment was used for NSCs using Human Neural Stem Cell Immunocytochemistry Kit (Thermo Fisher Scientific). To assess the neural stemness of the cells, the neuronal markers Nestin, SOX2, SOX1, and PAX6 were detected. Neurons were differentiated for further 7 days. NSCs characterization is reported in (Carelli et al., 2019; Fantini et al., 2019; Scarian et al., 2022).

2.4. Cell culture

SH-SY5Y human neuroblastoma cells were cultured in DMEM/F12 Complete Medium supplemented with 10% of Fetal Bovine Serum (FBS; Euroclone), 1% glutamine (L-GLUT; GIBCO) and 1% Penicillin/Streptomycin (P/S, GIBCO) at 37 °C in a 5% CO_2. Retinoic acid (RA) was administered to differentiate the cells at a concentration of 10 μM for 7 days in a 1% FBS DMEM High Glucose medium to induce differentiation (Filograna et al., 2015).

2.5. Cell transfection

Lipofectamine® RNAiMAX (Invitrogen, USA) was used to obtain silencing of the ZEB1-AS1 gene. Specifically, two short interfering RNAs (siRNAs) were used to inhibit the expression of ZEB1-AS1 (siZEB1-AS1–1 id: n271645; siZEB1-AS1–2 id: n271641; Thermo Fisher Scientific) negative control was designed by using an un-specific siRNA (Thermo Fisher Scientific). The cells were 60–80% confluent at the time of transfection and the Lipofectamine® RNAiMAX reagent was diluted in the appropriate volume of Opti-MEM® Medium (Thermo Fisher Scientific). After that, cells were incubated for 72 h at 37 °C in a CO_2 incubator. For differentiated cells, silencing was performed at day 4 of differentiation and cells were incubated with the siRNA/lipofectamine complex for a further 72 h.

2.6. RNA extraction and real time PCR

Total RNA from PBMCs, SH-SY5Y cells, NSCs and neurons was extracted using TRIZOL® reagent (Thermo Fisher Scientific) following the manufacturer's instructions, and then quantified using the Multiskan GO spectrophotometer (Thermo Fisher Scientific). In this study, 500 ng of RNA were retro transcribed using the *iScript™ Reverse Transcription Supermix for RT-qPCR* (Bio-Rad) kit following manufacturer's instructions. Real-Time PCR was performed with the CFX Connect Real-Time PCR System (Bio-Rad) using SsoAdvanced™ Universal SYBR ® Green Supermix (Bio-Rad). The NCBI's Primer-BLAST tool was used to design primers. Gene expression was calculated using the $2^{-\Delta\Delta Ct}$ method. GAPDH was used as endogenous control. The list of primer used in this study is reported in Supplementary Table 1. For hsa-miR-200c and hsa-miR-139 Real time PCR analysis, the miRCURY LNA miRNA SYBR® Green PCR System (Qiagen) was used.

2.7. Western blotting analysis

Protein extracts of PBMCs and SH-SY5Y cells were obtained by means of RadioImmunoPrecipitation Assay (RIPA) lysis buffer (Carelli et al., 2019). Then, proteins were quantified with the Bradford Assay following standard protocol (Coomassie Plus—The Better Bradford Assay™ Reagent, Thermo Scientific). Equal amounts of solubilized proteins were heated in Laemmli sample buffer (Bio-Rad) containing 70 mM 2-β-mercaptoethanol (Sigma Aldrich), separated by SDS-PAGE gel 6% or 10% (depending on the molecular weight of investigated proteins) and electroblotted onto a nitrocellulose membrane (Trans-blot, Bio-Rad). Membranes were then fixed with 4% paraformaldehyde in 0.1 M PBS (Thermo Fisher Scientific), pH 7.4, for 30 min at room temperature, and then blocked in 5% slim milk (diluted in TBS with 0.05% Tween-20). After that, membranes were probed with the appropriate primary antibody: polyclonal anti-ZEB1 (1:1000; Abcam, ab124512), monoclonal anti-β-Catenin (1:1000; Immunological Sciences, MAB-94627), anti-BMI1 (1:500; Santa Cruz, SC390443), anti-GSK3β (1:500; Santa Cruz, SC377213), monoclonal anti-p-GSK3β (1:1000; Immunological Sciences, MAB-94624), monoclonal anti-GAPDH (GAPDH 1:1000; Cell Signaling, #2118), anti-vinculin (1:1000; abcam ab129002), overnight at 4 °C. Lastly, membranes were incubated with a specific secondary antibody Peroxidase AffiniPure Goat Anti-Rabbit/Mouse IgG (1:5000 dilution; Jackson Immuno Research). Proteins were visualized by means of an enhanced chemiluminescence detection solution (Thermo Fisher Scientific). After acquisition by a GelDoc™ image capture system (Uvitec, Eppendorf), densitometric analysis of the bands was performed using the ImageJ software.

2.8. Immunocytochemistry

SH-SY5Y cells were seeded on ethanol-washed glass coverslips and cultured in a standard medium. Then, cells were fixed with 4% paraformaldehyde in 0.1 M PBS (Thermo Fisher Scientific), pH 7.4, for 20 min at room temperature, and then washed with PBS. The coverslips were incubated overnight at 4 °C in PBS containing 10% normal goat serum (NGS, Thermo Fisher Scientific), 0.3% Triton X-100 (BDH, VWR), and the appropriate primary antibody. The cells morphological features were assessed by immunocytochemistry with the following antibodies: monoclonal anti-β-Catenin (1:200; Immunological Sciences, MAB-94627), anti-β3-tubulin (1:200; Covance, MMS-435P25). Cells were

thoroughly rinsed with PBS and 10% NGS and reacted with the appropriate secondary antibody (Alexa Fluor® 488 and 546, Thermo Fisher Scientific) for 1.5 h. Nuclei were stained with DAPI at the final concentration of 1 μg/ml for 10 min. Glass coverslips were mounted using the FluorSave Reagent (Calbiochem) and analyzed by confocal microscopy (Confocal laser scanning microscopy platform Leica TCS SP8, Leica Microsystems). As control, the appropriate secondary antibody was administrated omitting the primary one (Alexa Fluor® 488 or 546, Thermo Fisher Scientific). B-Catenin aggregation was assessed with the AggreCount v1.13, the automated image analysis tool written in the ImageJ macro language for Fiji (Klickstein et al., 2020).

2.9. MTT assays

SH-SY5Y cells were seeded in a 96-well plate at 2×10^5 cells/well density. At the end of the silencing period, 10 μl MTT assay kit reagent (Merck) was added to each well, and cells were incubated for 3 h. MTT crystals were eluted with 100 μl of elution solution, composed of 4 mM HCl, 0.1% (*v/v*) NP40 all in isopropanol for 30 min. The relative absorbance was measured with EnSight™ multimode plate reader (PerkinElmer) at $\lambda = 570$ nm. The results are expressed as a percentage of the absorbance read in control cells (siNEG).

2.10. LIVE/DEAD viability assay

The LIVE/DEAD ® Viability Assay (Thermo Fisher Scientific) is a two-colour fluorescence cell viability assay based on the simultaneous determination of live and dead cells with two probes: Calcein AM and Ethidium homodimer (EthD-1). Calcein is retained within live cells, producing an intense uniform green fluorescence in live cells (ex/em ~495 nm/~515 nm). EthD-1 enters cells with damaged membranes and undergoes a 40-fold enhancement of fluorescence upon binding to nucleic acids producing a red fluorescence in dead cells (ex/em ~495 nm/~635 nm).

In order to assess cell viability, 0.5 μl of EthD-1 and 0.2 μl of Calcein were diluted in 1 ml of medium phenol red free and added to the cell culture. After a 1 h incubation, cells were fixed and analyzed at the fluorescence microscope (Leica DMIL LED, Leica Microsystems).

2.11. RNA subcellular compartmentalization

To assess the RNAs intracellular localization cells were lysed in buffer A (Tris HCl pH 7 10 mM, NaCl 140 mM, $MgCl_2$ 1,5 mM, NP40 0,5%) and incubated on ice for 5 min. Cells were then centrifuged for 3 min at 1000*g* at 4 °C and the supernatant, containing the cytoplasmatic fraction, was then transferred. The pellet was washed three times with Lysis Buffer A and then incubated with Lysis Buffer B (Tris HCl pH 7 10 mM, NaCl 140 mM, $MgCl_2$ 1,5 mM, NP40 0,5%, Tween 20 1%, Deoxycholic acid 0,5%) and immediately centrifuged for 3 min at 1000*g* at 4 °C. The pellet containing the nuclear fraction was then collected for subsequent RNA extraction.

2.12. Statistical analysis for in vitro experiments

Statistics was evaluated using GraphPad Prism 8.0a version (GraphPad Software Inc). When two conditions were analyzed, Student's unpaired *t*-test was used. For all in vitro experiments, data are reported as mean ± Standard Error Mean (SEM). The level of statistical significance was set at $p = 0.05$.

3. Results

3.1. Investigation of a ZEB1-AS1 and related pathway in PBMCs and NSCs/neurons

ZEB1-AS1 is a lncRNA transcribed from a shared bi-directional promoter with its sense gene *ZEB1*, found down-regulated in PBMCs of sALS patients (Gagliardi et al., 2018). Since the mechanism of action of ZEB1-AS1 in the central nervous system is yet to be characterized, and ZEB1 RNA expression was found not to change in PBMCs of sALS patients (Gagliardi et al., 2018), we firstly investigated if ZEB1-AS1 canonical targets found in cancer cells are also affected in PBMCs from sALS patients compared to healthy controls (CTR). To this end, RNA expression level of hsa-miR-200c, BMI1, GSK3β and CTTNB1, the gene coding for β-Catenin, were measured in PBMCs of both sALS patients ($N = 10$) and healthy subjects ($N = 10$). This analysis showed that in sALS condition hsa-miR-200c and GSK3β are upregulated while BMI1 is coherently downregulated (Fig. 1A). Next, we evaluated ZEB1, BMI1, GSK3β, p-GSK3β and β-Catenin protein expression. This analysis showed no significant changes in protein expression, though BMI1 shows a decreasing trend, whilst a trend towards an increased expression was observed for the other proteins (Fig. 1B-C).

To better understand the role of ZEB1-AS1 in sALS, we set out to study its mechanism of action in iPSCs-derived NSCs and in neurons at 7 days after NSCs differentiation start. ZEB1-AS1, GSK3β and CTTNB1 genes are less expressed in NSCs derived from sALS patients compared to controls, whilst hsa-miR-200c expression is almost 3 times higher in sALS subjects (Fig. 1D). Interestingly, in this case GSK3β gene expression was reduced, suggesting that this pathway could have different mechanism in each specific cellular context analyzed. No significant variations for the same genes were evident in neurons instead (Fig. 1E). We thus hypothesized here a new potential mechanism of action of ZEB1-AS1 in sALS. Specifically, ZEB1-AS1 down-regulation directly leads to miR-200c overexpression that results in the inhibition of BMI1, one of its targets in sALS.

3.2. Characterization of ZEB1-AS1 downstream pathway in undifferentiated SH-SY5Y cells

In order to get more insights into the regulatory events downstream to ZEB1-AS1, its decrease was induced via RNA interference in the neuroblastoma cell line SH-SY5Y (siZEB1-AS1). Interestingly, ZEB1-AS1 interference increased mortality (Fig. 2A). Next, we studied the subcellular localization of ZEB1-AS1 since lncRNAs can have different actions according to their subcellular localization. GAPDH resulted increased in the cytoplasm, and U6 in the nucleus as expected. Moreover, results highlight that ZEB1-AS1 distribution is ubiquitous in SH-SY5Y cells, possibly with a slight predominance in the cytoplasm (Fig. 2B). Importantly, ZEB1-AS1 silencing does not significantly influence ZEB1 expression but leads to an increase of hsa-miR-200c coherently to what already observed in PBMCs and NSCs derived from sALS subjects (Fig. 1A, Fig. 1D). Consequently, up-regulation of hsa-miR-200c causes a significant downregulation of BMI1 and a significant increase of GSK3β levels while a non-significant increase in CTTNB1 mRNA expression (Fig. 2C). Protein expression levels of ZEB1-AS1's downstream targets were detected by WB and the results show that siZEB1-AS1 interfered cells express less ZEB1 as well as BMI1 whilst p-GSK3β is increased, along with the p-GSK3β/GSK3β ratio (Fig. 2D). In addition, the data show that GSK3β manifests a trend of increased expression, whilst β-Catenin levels remain constant (Fig. 2D).

3.3. Implications for ZEB1-AS1 in SH-SY5Y neural differentiation

Since the affected cells in ALS are mainly post-mitotic cells, undifferentiated SH-SY5Y cells were treated with retinoic acid (RA) for 7 days to induce neuronal differentiation as already reported, with an increased expression in neuronal markers MAP2, TUJ and NESTIN (Supplementary Fig. 1) (Encinas et al., 2000). Results highlighted an increase in ZEB1-AS1 and ZEB1 expression in differentiated cells, along with a concordant increase in BMI1 and CTTNB1 (Fig. 3A). Interestingly, ZEB1-AS1 silencing during differentiation leads to a slight increase in both MAP2 and TUJ RNAs expression, both markers of mature neurons while

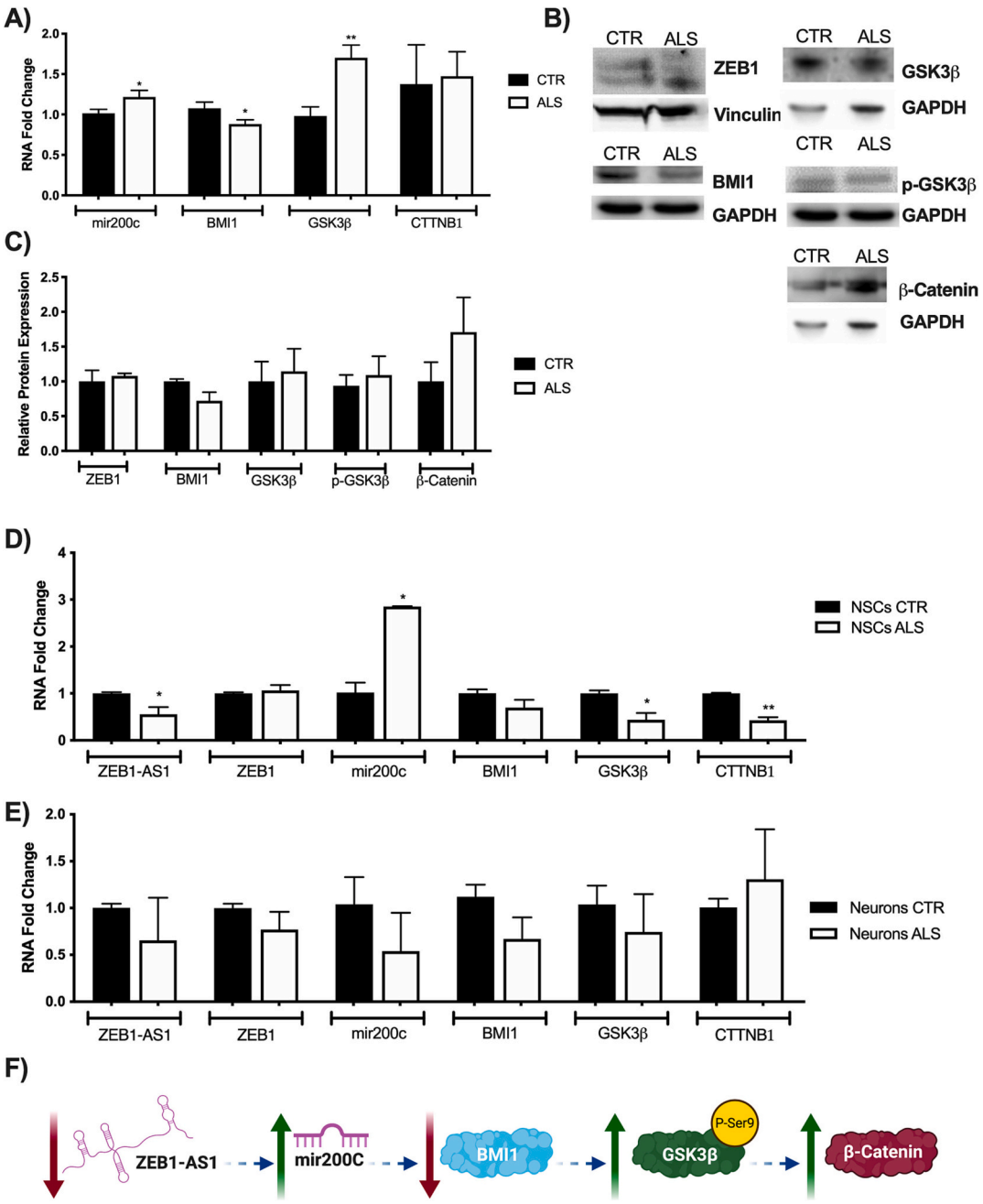

Fig. 1. Investigation of ZEB1-AS1's mechanism of action in ex vivo models (A) Assessment of RNA expression levels of ZEB1-AS1 possible target molecules in PBMCs. GAPDH was used as housekeeping gene. Data are expressed as means ± SEM ($N = 10$; *$p < 0.05$, **$p < 0.01$ vs CTR). Protein analysis of ZEB1-AS1 possible downstream targets in PBMCs. Western Blot (B) and relative protein quantification (C) of ZEB1, BMI1, GSK3β, p-GSK3β and β-Catenin in PBMCs from CTR and sALS patients. Proteins were normalized against GAPDH for low-molecular weight proteins, and against Vinculin for high molecular weight proteins (ZEB1 and β-Catenin). Data are expressed as means ± SEM ($N \geq 5$, *p < 0.05 vs CTR). (D) Analysis of ZEB1-AS1 and target genes expression in neural stem cells from sALS patients (NSCs ALS) and control subjects (NSCs CTR). GAPDH was used as housekeeping gene. Data are expressed as means ± SEM ($N = 3$). E) Analysis of ZEB1-AS1 and target genes expression in neurons from sALS patients (Neurons ALS) and control subjects (Neurons CTR). GAPDH was used as housekeeping gene. Data are expressed as mean ± SEM (N = 3 independent experiments performed in iPSCs from 1 CTRL and 1 sALS patient respectively).

NESTIN was unchanged (Fig. 3B). TUJ protein also shows a tendency to increase as reported via immunofluorescence (Fig. 3C) and western blot analysis (Fig. 3D). Moreover, we confirmed that CTTNB1 protein product β-Catenin is increased during differentiation (Fig. 3E) and we propose this could be due to a regulation performed by hsa-miR-139, as this miRNA presents a reduced expression during differentiation and was found to modulate β-Catenin (Hawkins et al., 2022) (Fig. 3F).

With these results in mind, it was relevant to characterize the implication of ZEB1-AS1 silencing in differentiated SH-SY5Y. Interestingly, results prove that ZEB1-AS1 down-regulation does not significantly affect cellular mortality of differentiated SH-SY5Y cells (Fig. 4A). Moreover, ZEB1-AS1 presents a ubiquitous localization in this cellular context (Fig. 4B). RNA expression analysis following ZEB1-AS1 knock-down still showed an increase in hsa-miR-200c and a decrease in BMI1 (Fig. 4C), but interestingly protein expression analysis showed a decrease in β-Catenin expression (Fig. 4D). Remarkably, hsa-miR-139 expression was increased and this could explain β-Catenin decrease in expression (Fig. 4E).

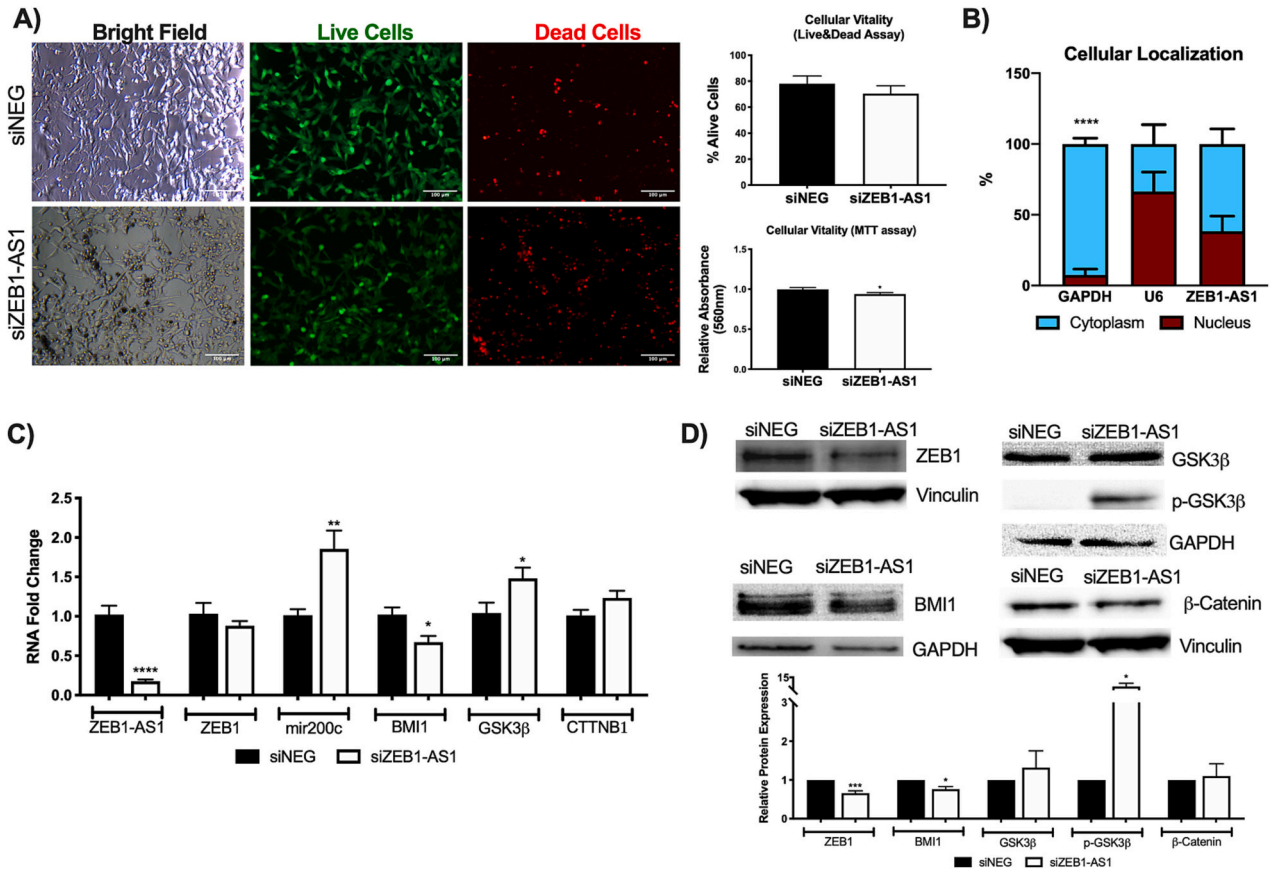

Fig. 2. Effect of ZEB1-AS1 silencing in undifferentiated SH-SY5Y. (A) Effect of ZEB1-AS1 silencing on cell vitality. Live&Dead assay with representative images of live cells (green) and dead cells (red) and relative histogram of % of alive cells (Top histogram) Data are expressed as mean ± SEM of 4 fields analyzed per 3 independent experiments ($N = 12$). The bottom histogram shows MTT assay in siNEG and siZEB1-AS1 conditions. Data are expressed as mean ± SEM of 8 wells of 3 independent experiments ($N = 24$, $^{*}p < 0.01$ vs siNEG). (B) Assessment of ZEB1-AS1 cellular localization. Data are expressed as mean ± SEM of 3 independent experiments performed in duplicate ($N = 6$, $^{****}p < 0.001$ cytoplasmic vs nuclear expression). (C) RNA relative quantification of ZEB1-AS1 and its possible targets in siNEG and siZEB1-AS1 conditions. Data are expressed as mean ± SEM of 3 independent experiments performed in duplicate (N = 6; $^{*}p < 0.05$, $^{**}p < 0.01$, $^{****}p < 0.0001$ vs siNEG). (D) Western Blot analysis (top) and protein quantification (bottom) of ZEB1, BMI1, GSK3β, p-GSK3β, p-GSK3β/GSK3β and β-Catenin in siNEG and siZEB1-AS1 conditions. Proteins were normalized against GAPDH for low-molecular weight proteins, and against Vinculin for high molecular weight proteins (ZEB1 and β-Catenin). Data are expressed as mean ± SEM ($N \geq 4$, $^{*}p < 0.05$, $^{***}p < 0.001$ vs siNEG). (For interpretation of the references to colour in this figure legend, the reader is referred to the web version of this article.)

3.4. Implications of ZEB1-AS1 silencing on β-Catenin

Recent evidence suggests that GSK3β directly affects neural progenitors differentiation into neural phenotype by titrating the levels of β-Catenin in ALS (Choi et al., 2020). Moreover, increased levels in GSK3β lead to β-Catenin accumulation in the cytoplasm where it creates insoluble protein aggregates which are considered hallmarks of sALS (Pinto et al., 2019). Thus, we wanted to understand the impact of ZEB1-AS1's expression in the formation of β-Catenin structures in cytosolic, perinuclear and nuclear compartments in both undifferentiated and differentiated SH-SY5Y cells silenced for ZEB1-AS1 expression versus their respective control (siNEG). Results demonstrate that in undifferentiated SH-SY5Y there is a significative decrease of cytoplasmic and peri-nuclear β-Catenin structures formation in siZEB1-AS1 with respect to siNEG, whilst interestingly the opposite is true in differentiated SH-SY5Y cells (Fig. 5A, Supplementary Fig. 2). Moreover, the cytosolic/nuclear and perinuclear/nuclear ratio of structures intensity is abundantly increased in differentiated SH-SY5Y silenced for ZEB1-AS1 expression (Fig. 5B).

Neurite elongation and branching are crucial cellular events that occur during differentiation to neuronal cells. They are specialized cytoplasmic domains whose formation depends on the presence of external cues and of intracellular mechanisms comprising β-Catenin signaling pathway (Endo et al., 2008). We thus assessed neurite length by TUJ immunostaining in SH-SY5Y cells silenced for ZEB1-AS1 at 4 days post differentiation start. The results demonstrate that in siZEB1-AS1 interfered cells the average neurite length decreases in differentiated cells confirming the role of ZEB1-AS1 in the determination of the neural phenotype (Fig. 5C). We thus propose that ZEB1-AS1 has a different and specific mechanism of action in undifferentiated and differentiated cells, leading to the alteration of β-Catenin signaling pathway (Fig. 6.)

4. Discussion

ALS is a progressive neurodegenerative in which the dysregulation in RNA-binding proteins, in gene expression and in transcription factors activities appears to play a crucial role, along with alterations in lncRNAs expression and mechanism of action (Garofalo et al., 2020; Riva et al., 2016; Gagliardi et al., 2018; Rey et al., 2021d). Previous studies also proposed an involvement of oncogenic pathways in cancer and neurodegenerative diseases underlining the hypothesis that the same oncogene could play a role in two different pathogenetic mechanisms (Rey et al., 2021d; Pandini et al., 2021). The oncogenic lncRNA ZEB1-AS1 was previously found amongst the TOP 10 deregulated genes in PBMCs of sALS patients as opposed to healthy control patients

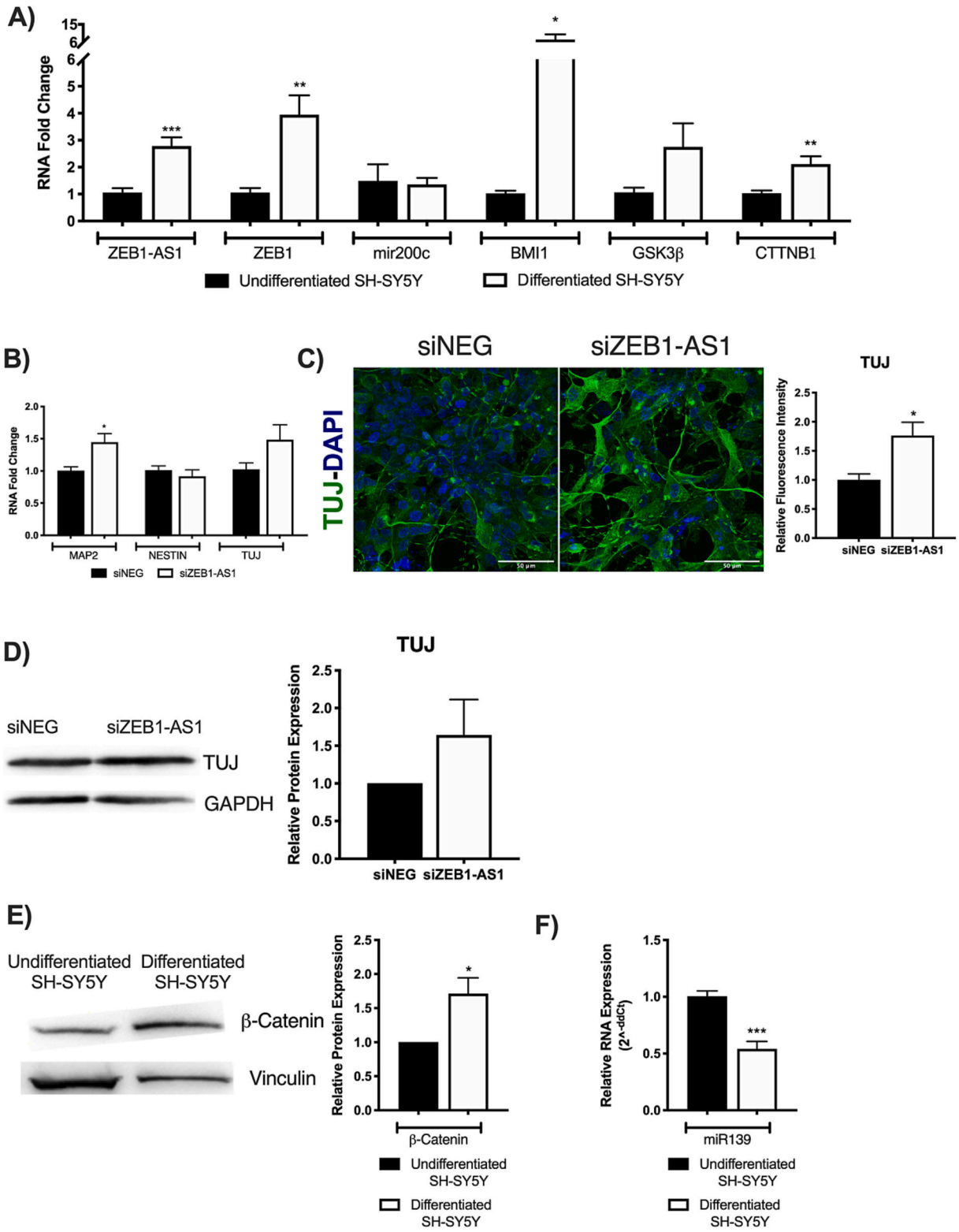

Fig. 3. Implications for ZEB1-AS1 on neural differentiation. (A) RNA relative quantification of ZEB1-AS1 and its possible targets during SH-SY5Y differentiation. Data are expressed as mean ± SEM of 3 independent experiments performed in duplicate ($N = 6$; *$p < 0.05$, **$p < 0.01$, ***$p < 0.001$ vs Undifferentiated SH-SY5Y). (B) RNA relative quantification of neural differentiation markers in differentiated SH-SY5Y silenced for ZEB1-AS1 expression (siZEB1-AS1) versus control (siNEG). Data are expressed as mean ± SEM 3 independent experiments performed in duplicate ($N = 6$, *$p < 0.05$ vs siNEG). (C) Immunocytochemistry of TUJ under ZEB-1-AS1 silencing (siZEB1-AS1) vs control (siNEG); nuclei are stained with DAPI, scale bar 50 μm (left). Analysis of TUJ relative fluorescence was performed with ImageJ. Data are expressed as mean ± SEM. 3 fields per experiment from 3 independent experiments were analyzed. ($N = 9$, *p < 0.05 vs siNEG). (D) Western Blot analysis (left) and protein quantification (right) of TUJ in siNEG and siZEB1-AS1 conditions. Proteins were normalized against GAPDH Data are expressed as mean ± SEM ($N = 4$). (E) Western Blot analysis (left) and protein quantification (right) of β-Catenin during SH-SY5Y differentiation. Proteins were normalized against Vinculin. Data are expressed as mean ± SEM ($N = 3$, *p < 0.05 vs siNEG) (F) RNA relative quantification of miR139 during SH-SY5Y differentiation. Data are expressed as mean ± SEM of 3 independent experiments performed in duplicate (N = 6; ***$p < 0.001$ vs Undifferentiated SH-SY5Y)..

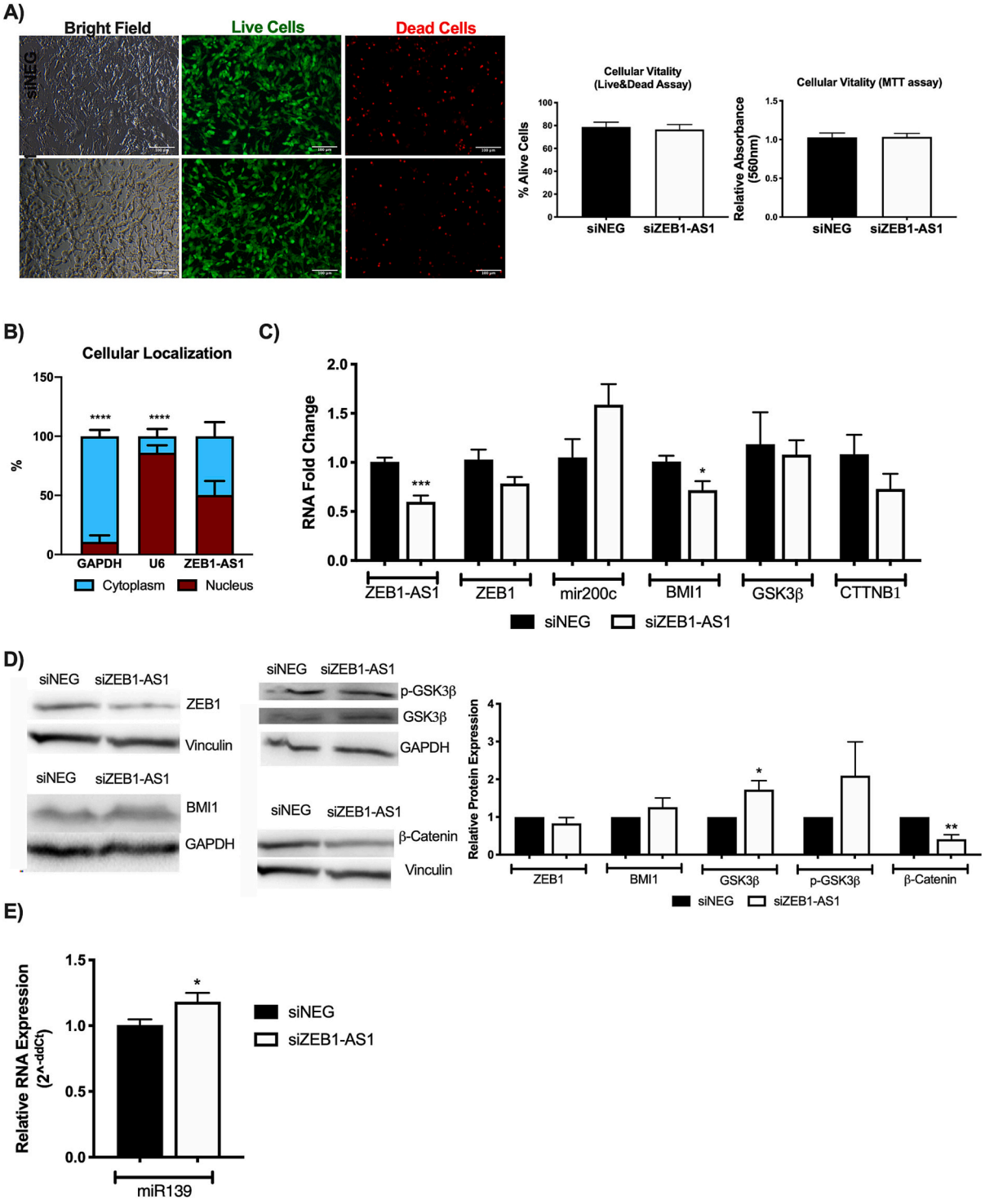

Fig. 4. Effect of ZEB1-AS1 silencing in differentiated SH-SY5Y. (A) Effect of ZEB1-AS1 silencing on cell vitality. Live&Dead assay with representative images of live cells (green) and dead cells (red) and relative histogram of % of alive cells (left histogram) Data are expressed as mean ± SEM of 4 fields analyzed per 3 independent experiments ($N = 12$). The right histogram shows MTT assay in siNEG and siZEB1-AS1 conditions. Data are expressed as mean ± SEM of 8 wells of 3 independent experiments ($N = 32$). (B) Assessment of ZEB1-AS1 cellular localization. Data are expressed as mean ± SEM of 3 independent experiments performed in duplicate ($N = 6$, $^{****}p < 0.001$ cytoplasmic vs nuclear expression). (C) RNA relative quantification of ZEB1-AS1 and its possible targets in siNEG and siZEB1-AS1 conditions. Data are expressed as mean ± SEM of 3 independent experiments performed in duplicate (N = 6; $^{*}p < 0.05$, $^{***}p < 0.001$ vs siNEG). (D) Western Blot analysis (top) and protein quantification (bottom) of ZEB1, BMI1, GSK3β, p-GSK3β and β-Catenin in siNEG and siZEB1-AS1 conditions. Proteins were normalized against GAPDH for low-molecular weight proteins (BMI1, GSK3β and p-GSK3β), and against Vinculin for high molecular weight proteins (ZEB1 and β-Catenin). Data are expressed as mean ± SEM ($N = 4$, $^{*}p < 0.05$, $^{**}p < 0.01$ vs siNEG). (E) RNA relative quantification of miR139 following ZEB1-AS1 silencing. Data are expressed as mean ± SEM of 3 independent experiments performed in duplicate (N = 6; $^{*}p < 0.05$ vs siNEG). (For interpretation of the references to colour in this figure legend, the reader is referred to the web version of this article.)

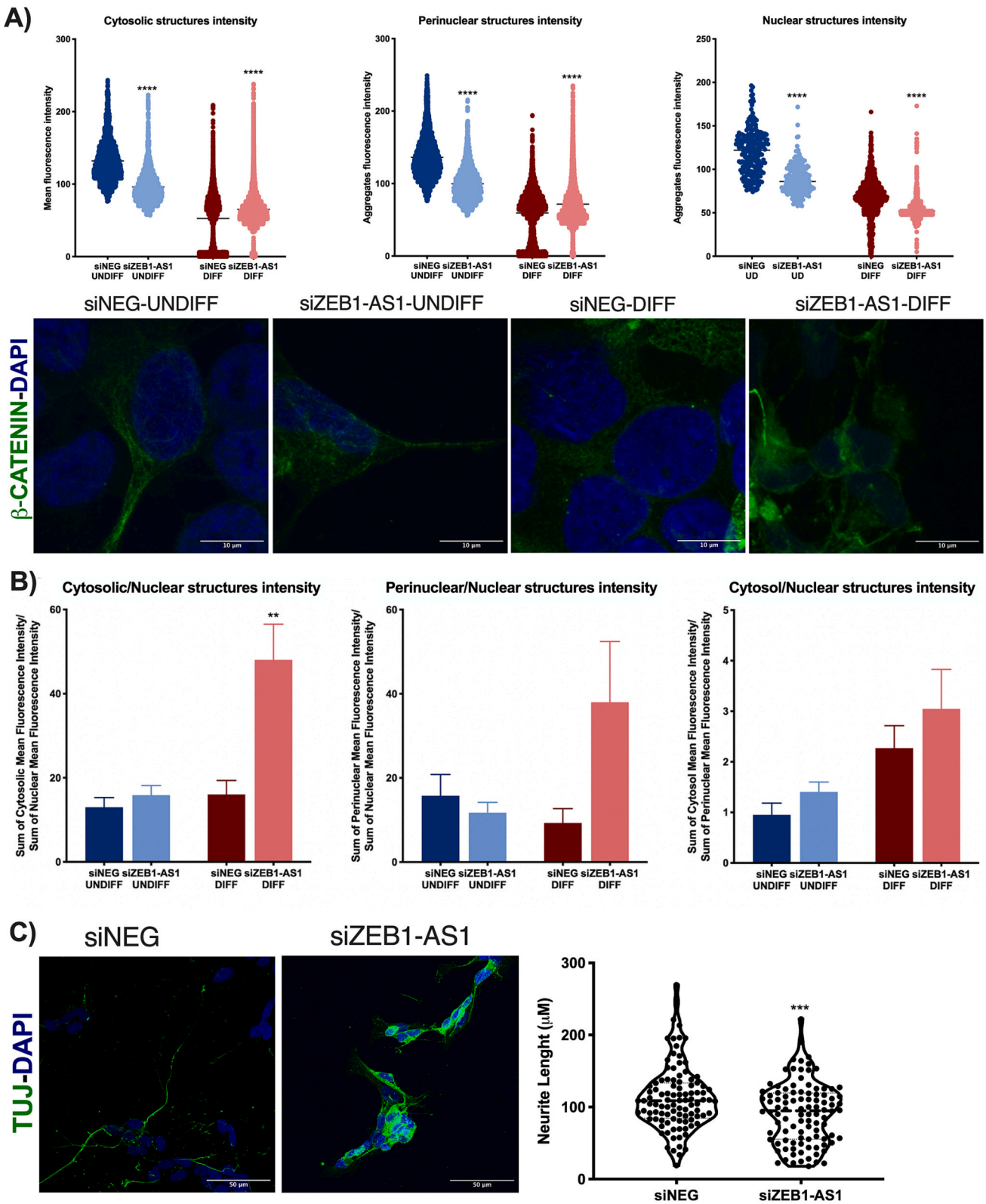

Fig. 5. Implications for ZEB1-AS1 silencing on β-Catenin structures formation and functionality. (A) Analysis of β-Catenin structures in cytosolic, perinuclear and nuclear compartments in undifferentiated and differentiated SH-SY5Y treated with mock siRNA (siNEG) or with ZEB1-AS1 siRNA (siZEB1-AS1). Quantification of structures intensity was performed with AggreCount. 3 fields per experiment from 3 independent experiments were analyzed (****$p < 0.0001$ vs siNEG). (top) representative images of immunocytochemistry analysis of β-Catenin under ZEB1-AS1 silencing (siZEB1-AS1) vs control (siNEG) in undifferentiated and differentiated SH-SY5Y. Nuclei are stained with DAPI. Scale bars = 25 µm (B) Ratio of β-Catenin structures when considering cytosolic/nuclear, perinuclear/nuclear and cytosolic/perinuclear structures intensity. Quantification of structures intensity was performed with AggreCount. 3 fields per experiment from 2 independent experiments were analyzed (**$p < 0.01$ vs siNEG). (C) Neurite length analysis: Immunocytochemistry of TUJ under ZEB-1-AS1 silencing (siZEB1-AS1) vs control (siNEG); nuclei are stained with DAPI, scale bar 50 µm (left). Analysis of neurite length was performed with ImageJ. Data are expressed as mean ± SEM. 3 fields per experiment from 3 independent experiments were analyzed, 10 neurites were analyzed per field. ($N = 90$, ***p < 0.0001 vs siNEG).

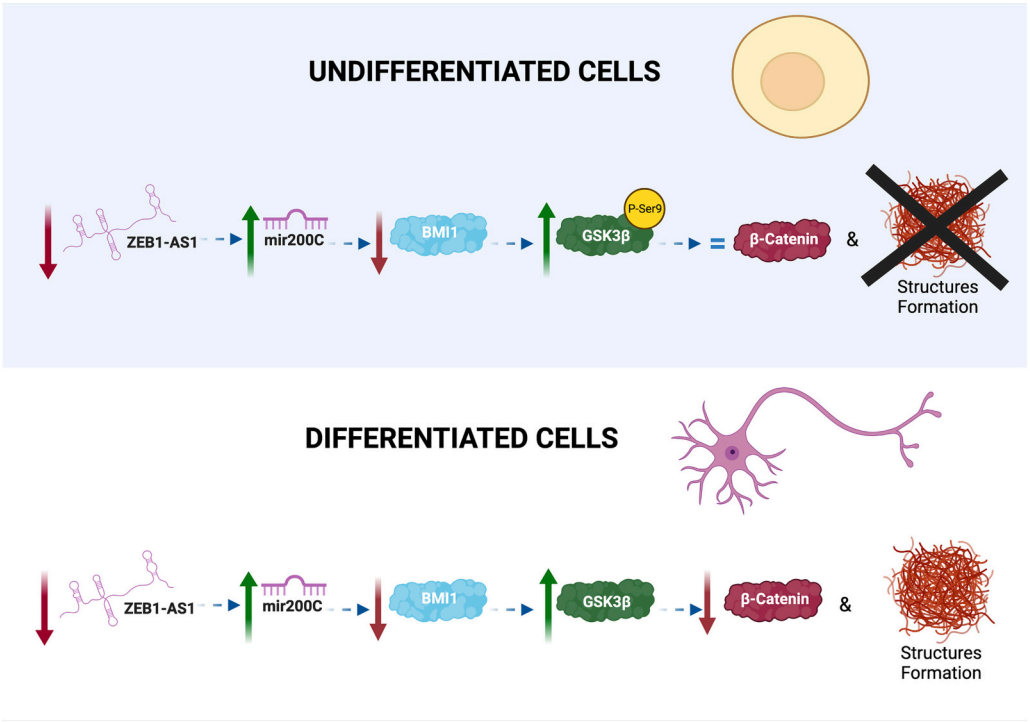

Fig. 6. Suggested mechanism of action of ZEB1-AS1 decrease in neuronal cell maturation. In undifferentiated cells, ZEB1-AS1 decrease ultimately leads to steady levels of β-Catenin, without the formation of structures. In differentiated neuronal cells, soluble β -Catenin appears to decrease with a concomitant increase in structures formation. Created with Biorender.com

(Gagliardi et al., 2018), and the aim of this work was thus to investigate the mechanism of action of the antisense lncRNA ZEB1-AS1 in relation to sALS.

To characterize the cellular context in which ZEB1-AS1 was first found dysregulated, we investigated a previously reported pathway involving ZEB1-AS1, highlighting an inverse correlation between ZEB1-AS1 and hsa-miR-200c (Gagliardi et al., 2018; Fu et al., 2019), which was also confirmed in sALS-derived iPSCs differentiated to NSCs. As we found that the impact of ZEB1-AS1 on his down-stream targets GSK3β and β-Catenin (Pinto et al., 2019; Flamier et al., 2018) was different in PBMCs and NSCs, we hypothesized that this could be due to the different cellular phenotype and we thus set out to analyze the plausibility of this hypothesis in relation to ZEB1-AS1 decreased expression in cells with a neural phenotype.

Specifically, the effect of ZEB1-AS1 silencing in the SH-SY5Y cell line was assessed in both undifferentiated and differentiated conditions and the results highlight that ZEB1-AS1 mechanism of action may influence multiple levels of gene expression thus resulting in complex and different phenotypes. Indeed, the final impact of ZEB1-AS1 on β-Catenin was not always linear, as this protein was found to remain stable when ZEB1-AS1 was silenced in undifferentiated cells; whilst it decreased when ZEB1-AS1 was silenced in differentiated SH-SY5Y. β-Catenin is phosphorylated by GSK3β and subsequently degraded, thus GSK3β phosphorylation observed after ZEB1-AS1 silencing may influence β-Catenin's mechanism of action. Moreover, there could also be a regulation of the protein by hsa-miR-139, previously found to target β-Catenin (Hawkins et al., 2022), which could connect ZEB1-AS1 with the mechanism proposed recently by Hawkins and co-workers for the motor neurons death in both FUS and sporadic ALS (Hawkins et al., 2022). ZEB1-AS1 could also act on different β-Catenin partners, not only GSK3β, which might play different roles in the different stages of neural differentiation. Indeed, the protein increases during differentiation, suggesting it could play different roles depending on the cellular stage of differentiation (Israsena et al., 2004). The protein was also found to form peculiar "structures" of increased intensity when ZEB1-AS1 was inhibited in differentiated cells. Specifically, the patterns-formation for these β-Catenin structures were opposed, with a decreased cytosolic and perinuclear structures formation in undifferentiated SH-SY5Y cells silenced for ZEB1-AS1 expression with respect to siNEG, and an opposite pattern in differentiated SH-SY5Y. In particular, the cytosolic/nuclear structure ratio and the perinuclear/nuclear structures ratio appears to be increased in differentiated SH-SY5Y silenced for ZEB1-AS1. This observation is in line with increased levels in GSK3β which lead to β-Catenin accumulation in the cytoplasm where it has been shown to contribute to insoluble protein aggregation and inclusion bodies formation, both hallmarks of several neurodegenerative diseases such as ALS (Pinto et al., 2019). Although we cannot confirm this mechanism in our cellular context for a lack of characterization of these structures, future works should focus on the assessment of these inclusions through an analysis of their co-localization with aggresomes, stress granules, amyloid aggregates and SDS-resistant protein species (Pinto et al., 2019).

ZEB1-AS1 may thus play a different role in different phases of the neural differentiation process, and indeed we found the lncRNA to have an impact on the expression of neural-related markers (MAP2 and TUJ). One strategy to decipher the molecular mechanisms affecting motor neuron loss in ALS is by looking for factors with active roles during motor neuron development such as neurite elongation and branching whose formation depends on the interaction of external cues and intracellular mechanisms (Birger et al., 2018). Although this was not strictly possible in our SH-SY5Y cellular model, we report that β-Catenin structures formation also leads to a decreased neurite length, suggesting this could be a read out of ZEB1-AS1 silencing. It is intriguing to link our experimental results to the observation that in ALS-related pathology and in most of sALS cases neurons develop shorter neurites, as found when ZEB1-AS1 expression is decreased (Osking et al., 2019; Kikuchi et al., 1999). Even so, there is a need, in the near future, to assess this mechanism in neuronal cells to validate this mechanism with certainty. Our work provides a first characterization of the implication of ZEB1-AS1 in sALS pathogenesis and neural differentiation. Further experiments will surely be needed to deeply eviscerate the proposed

mechanism, as the difficulty to retrieve neural cells and the limited yield of neurons from iPSCs-differentiation surely represent a limitation. Moreover, a direct study of β-Catenin solubility following ZEB1-AS1 silencing is surely needed to assess the possible pathogenicity of this lncRNA.

In future works, it will be extremely interesting to characterize whether the inhibition of ZEB1-AS1 in iPSCs-derived neural stem cells causes a cellular development alteration resembling the sALS phenotype, and/or whether this has implication on the β-Catenin pathway.

5. Conclusions

In conclusion, this study proposes a new pathway that elucidates the role of the lncRNA ZEB1-AS1 in relation neural differentiation in ALS, highlighting a relevant role for β-Catenin functionality. Our study highlights a role in cytoplasmic signal transduction for the molecule, as RNA interference typically affects lncRNAs expression in this compartment, and further inhibitory approaches could be of use in the characterization of ZEB1-AS1 mechanism of action. Even so, our study represents a first, relevant, characterization of ZEB1-AS1 signal transduction in ALS pathology.

Supplementary data to this article can be found online at https://doi.org/10.1016/j.nbd.2023.106030.

Ethics approval and consent to participate

The study was conducted in accordance with the Declaration of Helsinki and approved by the Ethics Committee of IRCCS Mondino Foundation for the preparation of PBMCs and iPSCs (p-20180034329).

Consent for publication

Not applicable.

Availability of data and material

Data sharing is not applicable to this article as no datasets were generated or analyzed during the current study.

Funding

This project was partially funded by Fondazione Regionale per la Ricerca Biomedica (TRANS-ALS; 2015–0023). GZ and SC are grateful to Pediatric Clinical Research Center Fondazione “Romeo ed Enrica Invernizzi” for its support. This project was partially funded by Italian Ministry of Health (RC2022–2023).

Authors’ contributions

FR: conceptualization, work design, data acquisition and interpretation, writing and revising of the manuscript; EM: data acquisition and interpretation, writing and revising of the manuscript; LM, LE, BB, CP, MB: data acquisition and interpretation; SG: data interpretation; MTR, GZ: funding acquisition, supervision; MM: data interpretation, revising of the manuscript; SC: conceptualization, work design, data interpretation, writing and revising of the manuscript, supervision, funding acquisition; CC: conceptualization, data interpretation, manuscript revision, supervision.

Declaration of Competing Interest

The authors declare that they have no competing interests.

Data availability

Data will be made available on request.

Acknowledgements

The authors are grateful to all participating patients and their families.

References

Armentero, M.T., Sinforiani, E., Ghezzi, C., Bazzini, E., Levandis, G., Ambrosi, G., et al., 2011. Peripheral expression of key regulatory kinases in Alzheimer’s disease and Parkinson’s disease. Neurobiol. Aging 32 (12).
Bensimon, G., Lacomblez, L., Meininger, V., 1994. A controlled trial of riluzole in amyotrophic lateral sclerosis. ALS/Riluzole study group. N. Engl. J. Med. 330 (9).
Birger, A., Ottolenghi, M., Perez, L., Reubinoff, B., Behar, O., 2018. ALS-related human cortical and motor neurons survival is differentially affected by Sema3A article. Cell Death Dis. 9 (3).
Carelli, S., Giallongo, T., Rey, F., Latorre, E., Bordoni, M., Mazzucchelli, S., et al., 2019. HuR interacts with lincBRN1a and lincBRN1b during neuronal stem cells differentiation. RNA Biol. 16 (10).
Choi, H.J., Cha, S.J., Lee, J.W., Kim, H.J., Kim, K., 2020. Recent advances on the role of gsk3β in the pathogenesis of amyotrophic lateral sclerosis. In: Brain Sciences, vol. 10.
Encinas, M., Iglesias, M., Liu, Y., Wang, H., Muhaisen, A., Ceña, V., et al., 2000. Sequential treatment of SH-SY5Y cells with retinoic acid and brain-derived neurotrophic factor gives rise to fully differentiated, neurotrophic factor-dependent, human neuron-like cells. J. Neurochem. 75 (3).
Endo, Y., Beauchamp, E., Woods, D., Taylor, W.G., Toretsky, J.A., Üren, A., et al., 2008. Wnt-3a and Dickkopf-1 stimulate neurite outgrowth in Ewing tumor cells via a Frizzled3- and c-Jun N-terminal kinase-dependent mechanism. Mol. Cell. Biol. 28 (7).
Fantini, V., Bordoni, M., Scocozza, F., Conti, M., Scarian, E., Carelli, S., et al., 2019. Bioink composition and printing parameters for 3D modeling neural tissue. Cells. 8 (8).
Filograna, R., Civiero, L., Ferrari, V., Codolo, G., Greggio, E., Bubacco, L., et al., 2015. Analysis of the catecholaminergic phenotype in human SH-SY5Y and BE(2)-M17 neuroblastoma cell lines upon differentiation. PLoS One 10 (8).
Flamier, A., El Hajjar, J., Adjaye, J., Fernandes, K.J., Abdouh, M., Bernier, G., 2018. Modeling late-onset sporadic Alzheimer’s disease through BMI1 deficiency. Cell Rep. 23 (9).
Fu, J., Peng, L., Tao, T., Chen, Y., Li, Z., Li, J., 2019. Regulatory roles of the miR-200 family in neurodegenerative diseases. Biomed. Pharmacother. 119.
Gagliardi, S., Zucca, S., Pandini, C., Diamanti, L., Bordoni, M., Sproviero, D., et al., 2018. Long non-coding and coding RNAs characterization in peripheral blood mononuclear cells and spinal cord from amyotrophic lateral sclerosis patients. Sci. Rep. 8 (1).
Garofalo, M., Pandini, C., Bordoni, M., Pansarasa, O., Rey, F., Costa, A., et al., 2020. Alzheimer’s, parkinson’s disease and amyotrophic lateral sclerosis gene expression patterns divergence reveals different grade of RNA metabolism involvement. Int. J. Mol. Sci. 21 (24).
Gianferrara, T., Cescon, E., Grieco, I., Spalluto, G., Federico, S., 2022. Glycogen synthase kinase 3β involvement in neuroinflammation and neurodegenerative diseases. Curr. Med. Chem. 29.
Hawkins, S., Namboori, S.C., Tariq, A., Blaker, C., Flaxman, C., Dey, N.S., et al., 2022. Upregulation of β-catenin due to loss of miR-139 contributes to motor neuron death in amyotrophic lateral sclerosis. Stem Cell. Rep. 17 (7), 1650–1665. Jul 12.
Hu, S., Begum, A.N., Jones, M.R., Oh, M.S., Beech, W.K., Beech, B.H., et al., 2009. GSK3 inhibitors show benefits in an Alzheimer’s disease (AD) model of neurodegeneration but adverse effects in control animals. Neurobiol. Dis. 33 (2).
Israsena, N., Hu, M., Fu, W., Kan, L., Kessler, J.A., 2004. The presence of FGF2 signaling determines whether β-catenin exerts effects on proliferation or neuronal differentiation of neural stem cells. Dev. Biol. 268 (1).
Jackson, C., Heiman-Patterson, T., Kittrell, P., Baranovsky, T., McAnanama, G., Bower, L., et al., 2019. Radicava (edaravone) for amyotrophic lateral sclerosis: US experience at 1 year after launch. Amyotroph. Lateral Scler Front. Degener. 20 (7–8).
Jia, L., Piña-Crespo, J., Li, Y., 2019. Restoring Wnt/β-catenin signaling is a promising therapeutic strategy for Alzheimer’s disease. In: Molecular Brain, vol. 12.
Kikuchi, H., Doh-ura, K., Kawashima, T., Kira, J.I., Iwaki, T., 1999. Immunohistochemical analysis of spinal cord lesions in amyotrophic lateral sclerosis using microtubule-associated protein 2 (MAP2) antibodies. Acta Neuropathol. 97 (1).
Klickstein, J.A., Mukkavalli, S., Raman, M., 2020. AggreCount: an unbiased image analysis tool for identifying and quantifying cellular aggregates in a spatially defined manner. J. Biol. Chem. 295 (51).
Li, T., Xie, J., Shen, C., Cheng, D., Shi, Y., Wu, Z., et al., 2016. Upregulation of long noncoding RNA ZEB1-AS1 promotes tumor metastasis and predicts poor prognosis in hepatocellular carcinoma. Oncogene. 35 (12).
Li, J., Liang, Z., Zheng, J., Zhang, X., Fu, J., 2017. Long noncoding RNA ZEB1-AS1 predicts an unfavorable prognosis of non-small lung cancer and regulates epithelial to mesenchymal transition through reducing ZEB1 expression. Int. J. Clin. Exp. Pathol. 10 (11).
Li, J., Li, Z., Leng, K., Xu, Y., Ji, D., Huang, L., et al., 2018. ZEB1-AS1: a crucial cancer-related long non-coding RNA. Cell Prolif. 51.
Li, N., Yang, T., Qian, Yu W., Liu, H., Qiao, C., Liu, C., 2019. The role of Zeb1 in the pathogenesis of morbidly adherent placenta. Mol. Med. Rep. 20 (3).
Lyu, Y., Bai, L., Qin, C., 2019. Long noncoding RNAs in neurodevelopment and Parkinson’s disease. In: Animal Models and Experimental Medicine, vol. 2.

Marchetti, B., Tirolo, C., L'Episcopo, F., Caniglia, S., Testa, N., Smith, J.A., et al., 2020. Parkinson's disease, aging and adult neurogenesis: Wnt/β-catenin signalling as the key to unlock the mystery of endogenous brain repair. Aging Cell 19.
Meng, L., Ma, P., Cai, R., Guan, Q., Wang, M., Jin, B.Z., 2018. Long noncoding RNA ZEB1-AS1 promotes the tumorigenesis of glioma cancer cells by modulating the miR-200c/141-ZEB1 axis. Am. J. Transl. Res. 10 (11).
Mutch, C.A., Schulte, J.D., Olson, E., Chenn, A., 2010. Beta-catenin signaling negatively regulates intermediate progenitor population numbers in the developing cortex. PLoS One 5 (8).
Osking, Z., Ayers, J.I., Hildebrandt, R., Skruber, K., Brown, H., Ryu, D., et al., 2019. ALS-linked SOD1 mutants enhance neurite outgrowth and branching in adult motor neurons. iScience. 11.
Pandini, C., Garofalo, M., Rey, F., Garau, J., Zucca, S., Sproviero, D., et al., 2021. MINCR: a long non-coding RNA shared between cancer and neurodegeneration. Genomics. 113 (6).
Pinto, C., Medinas, D.B., Fuentes-Villalobos, F., Maripillán, J., Castro, A.F., Martínez, A. D., et al., 2019. β-Catenin aggregation in models of ALS motor neurons: GSK3β inhibition effect and neuronal differentiation. Neurobiol. Dis. 130.
Recabarren-Leiva, D., Alarcón, M., 2018. New insights into the gene expression associated to amyotrophic lateral sclerosis. Life Sci. 193.
Rey, F., Pandini, C., Messa, L., Launi, R., Barzaghini, B., Zangaglia, R., et al., 2021a. α-Synuclein antisense transcript SNCA-AS1 regulates synapses- and aging-related genes suggesting its implication in Parkinson's disease. Aging Cell 20 (12).
Rey, F., Urrata, V., Gilardini, L., Bertoli, S., Calcaterra, V., Zuccotti, G.V., et al., 2021b. Role of long non-coding RNAs in adipogenesis: state of the art and implications in obesity and obesity-associated diseases. Obes. Rev. 22 (7).
Rey, F., Zuccotti, G.V., Carelli, S., 2021c. Long non-coding RNAs in metabolic diseases: from bench to bedside. Trends Endocrinol. Metab. 32.
Rey, F., Marcuzzo, S., Bonanno, S., Bordoni, M., Giallongo, T., Malacarne, C., et al., 2021d. Lncrnas associated with neuronal development and oncogenesis are deregulated in sod1-g93a murine model of amyotrophic lateral sclerosis. Biomedicines. 9 (7).
Riva, P., Ratti, A., Venturin, M., 2016. The long non-coding RNAs in neurodegenerative diseases: novel mechanisms of pathogenesis. Curr. Alzheimer Res. 13 (11).
Robberecht, W., Philips, T., 2013. The changing scene of amyotrophic lateral sclerosis. Nat. Rev. Neurosci. 14.
Scarian, E., Bordoni, M., Fantini, V., Jacchetti, E., Raimondi, M.T., Diamanti, L., et al., 2022. Patients' stem cells differentiation in a 3D environment as a promising experimental tool for the study of amyotrophic lateral sclerosis. Int. J. Mol. Sci. 23 (10). May 1.
Siena, Á.D.D., Plaça, J.R., Araújo, L.F., de Barros, I.I., Peronni, K., Molfetta, G., et al., 2019. Whole transcriptome analysis reveals correlation of long noncoding RNA ZEB1-AS1 with invasive profile in melanoma. Sci. Rep. 9 (1).
Su, W., Xu, M., Chen, X., Chen, N., Gong, J., Nie, L., et al., 2017. Long noncoding RNA ZEB1-AS1 epigenetically regulates the expressions of ZEB1 and downstream molecules in prostate cancer. Mol. Cancer 16 (1).
Valvezan, A.J., Klein, P.S., 2012. GSK-3 and Wnt signaling in neurogenesis and bipolar disorder. Front. Mol. Neurosci 5.
Van Damme, P., Robberecht, W., Van Den Bosch, L., 2017. Modelling amyotrophic lateral sclerosis: Progress and possibilities. DMM Disease Models and Mechanisms 10.
Wang, P., Mokhtari, R., Pedrosa, E., Kirschenbaum, M., Bayrak, C., Zheng, D., et al., 2017. CRISPR/Cas9-mediated heterozygous knockout of the autism gene CHD8 and characterization of its transcriptional networks in cerebral organoids derived from iPS cells. Mol. Autism. 8 (1).
Wu, Y.Y., Kuo, H.C., 2020. Functional roles and networks of non-coding RNAs in the pathogenesis of neurodegenerative diseases. J. Biomed. Sci. 27.
Wu, H.T., Zhong, H.T., Li, G.W., Shen, J.X., Ye, Q.Q., Zhang, M.L., et al., 2020. Oncogenic functions of the EMT-related transcription factor ZEB1 in breast cancer. J. Transl. Med. 18.
Yang, Y., 2012. Wnt signaling in development and disease. In: Cell and Bioscience, vol. 2.